Available online at www.sciencedirect.com
ScienceDirect
Trans. Nonferrous Met. Soc. China 22(2012) 1041−1050
Transactions of Nonferrous Metals Society of China
www.tnmsc.cn

Effects of T6 heat treatment on mechanical, abrasive and erosive-corrosive wear properties of eutectic Al−Si alloy

A. K. GUPTA[1], B. K. PRASAD[1], R. K. PAJNOO[2], S. DAS[1]

1. CSIR - Advanced Materials and Processes Research Institute, Bhopal-462026, India;
2. Central Institute of Agricultural Engineering (ICAR), Bhopal-462028, India

Received 23 September 2011; accepted 5 December 2011

Abstract: The abrasive and erosive-corrosive properties of eutectic Al−Si (LM6) alloy were studied. Microstructural features of the alloy were altered by controlling the T6 heat treatment parameter, and their influence on hardness, strength and elongation, and response of the samples in erosion-corrosion and abrasion conditions were studied. Characteristics of the Al−Si alloy samples were compared with those of Al conventionally used in agricultural machineries. Fabrication of a typical component using the Al−Si alloy was also explored in order to understand the feasibility of using the alloy system for the envisaged applications. The study suggests the response of the samples in different conditions to be greatly influenced by parameters like chemical composition, microstructural features and applied load, traversal distance and test environment. The performance of even the as cast Al−Si alloy is far superior to that of the conventional Al samples, while the T6 heat treated Al−Si alloy shows improved performance. Accordingly, the as-cast as well as T6 heat treated Al−Si alloy has potential for applications in agriculture as a replacement for the conventionally used Al.
Key words: Al−Si alloy; heat treatment; abrasion; erosion; corrosion

1 Introduction

Sowing refers to broadcasting of seeds into tilled soil at an optimum depth and distance. One of the popularly used machines for sowing and metering seeds and fertilizers is known as seed-cum-fertilizer drill. Fluted roller is an external force-feed device used in the mechanical system for uniformly dropping the desired amounts of seed and fertilizer (like urea and diammonium phosphate) into the field during the sowing operation. This becomes a critical component of the sowing machinery system and usually is fabricated by casting scrap Al in the name of 'commercial Al' into shape in the Indian subcontinent [1]. It was suggested that severe pitting damage occurs in the Al alloy component due to the presence of bicarbonate, chloride, copper salts and alkali hydroxide in the surrounding media and is comparatively more prone to corrosion by chemical attack of the fertilizer [2,3]. The mentioned factors cause the component to loose its dimensional accuracy, resulting into improper metering of seed and fertilizer, mechanical damage to the seed being processed, inter-row variation of seeding and non-uniform placing of fertilizer, thus adversely affecting the efficiency and crop yield [4]. Poor strength and high susceptibility of the conventional component material to abrasive wear and erosion-corrosion encountered during operation appear to be responsible for the poor performance of the component.

Al−Si alloys have widely been used as wear resistant materials in different engineering applications. They are somewhat lighter than Al and exhibit good castability characteristics, and wear and corrosion resistance [5−7]. Binary eutectic Al−Si alloys like LM6 are hard with fairly good strength properties. Their response to heat treatment remains limited to morphological modification of eutectic Si particles [8]. Further, their better wear and corrosion resistance and relatively lower cost than other Al−Si alloys present them as an effective substitute to soft and weak Al with a wide application potential in the agricultural sector. It may be mentioned that alloying Al with Si imparts a significant improvement in the casting characteristics because of low thermal coefficient of expansion. Si also makes electrolytic potential of aluminum more positive in solution that is responsible for the improvement in corrosion resistance [5]. The high hardness of Si particles [9] imparts wear resistance to Al and renders the Al−Si alloys immune to intercrystalline attack in most rural,

Corresponding author: B. K. PRASAD; E-mail: bkprasad@ampri.res.in
DOI: 10.1016/S1003-6326(11)61281-8

industrial and marine environments as structural components [6]. Shrinkage and gas porosity during solidification of Al−Si alloys are appreciably reduced [10] in view of improved fluidity imparted to the alloy system by Si. Eutectic Al−Si alloys possess the highest fluidity [11]. However, despite great potential, the possibilities of using Al−Si alloys have not been explored in agricultural applications to the best of our knowledge, where components like fluted rollers are conventionally fabricated by unorganized sectors using commercial Al with poorly defined composition and characteristics. Also, since erosion-corrosion and abrasion are quite frequently encountered by the agricultural components in operation, characterization of their response in such conditions becomes essential to effectively assess their capability. Heat treatment of binary Al−Si alloys, which essentially belongs to the category of non heat treatable version [12], and a study of its influence on the response of the alloy system makes it interesting from academic and technical standpoints. Optimization of heat treatment parameters like temperature and duration of treatment becomes another important aspect of concern that greatly controls the behaviour of materials.

In view of the above, an attempt is made in this study to examine the response of an eutectic Al−Si (LM6) alloy vis-a-vis the conventional Al used for agricultural applications in erosive-corrosive and abrasive conditions. The effects of parameters like ageing duration, applied load, traversal distance, test duration and environment are also investigated on the wear response of the samples. The influence of ageing duration during T6 heat treatment, thereby bringing about morphological changes in the eutectic Si particles, is also examined on hardness, tensile elongation and strength of the Al−Si alloy. The end objective of this investigation is to identify a material with improved quality and performance over the conventional Al that could have potential for use as agricultural machinery components like fluted rollers of a seed-cum-fertilizer drill used for sowing purposes.

2 Experimental

2.1 Sample preparation

Cylindrical (20 mm in diameter and 150 mm in length) and disc shaped castings (120 mm in diameter and 6 mm in thickness) of experimental Al−Si (LM6) alloy and conventional Al were prepared by liquid metallurgy route using cast iron moulds. The composition and density of the alloys are shown in Table 1. In order to explore the feasibility of making components, different assembly elements like feed cup, feed roller and feed-cut-off (Fig. 1) of fluted roller (sowing) system were also cast using metallic moulds and CO_2-silicate hardened green sand core.

Table 1 Composition and density of experimental Al alloys

Al alloy	Composition/%				Density/ ($g \cdot cm^{-3}$)
	Al	Cu	Si	Fe	
Conventional Al sample	Bal.	1.2	2.5	0.8	2.78
Eutectic Al−Si alloy (LM6)	Bal.	0.1	11.2	0.6	2.69

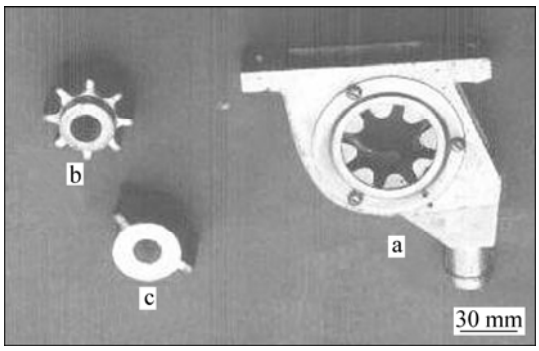

Fig. 1 Near net shape casting of fluted roller of Al−Si (LM6) alloy: (a) Feed cup; (b) Feed roller; (c) Feed cut off

2.2 Heat treatment

The Al−Si alloy was subjected to T6 heat treatment involving solutionizing followed by artificial ageing. The samples were solutionized at 525 °C for 3 h and quenched in water at ambient temperature. Ageing was carried out at 195 °C for 3−11 h. The aged samples were cooled in air to room temperature.

2.3 Abrasion tests

High stress abrasion tests were carried out on 35 mm×40 mm×3 mm rectangular specimens using a abrasion tester (Suga, Japan). The test essentially involves to-and-fro motion of the samples loaded against an abrasive medium. An abrasive paper fixed on a rotating metallic wheel served as the abrasive medium. The tests were carried out at the applied loads of 3 and 7 N while the abrasive employed was 180 grit (the corresponding particle size being 80 μm) SiC emery paper. Traversal distances adopted were 400, 800 and 1200 cycles corresponding to linear distances of 26, 52 and 78 m, respectively. Test arrangement was such that, by the time the specimen completed one to-and-fro movement/cycle, the abrasive wheel rotated one step forward enabling fresh abrasive surface to come in contact with the sample. Further, the wheel took one complete rotation by the time the specimen completed 400 to-and-fro movements/cycles. Each test was initiated using fresh abrasive medium, meaning thereby that fresh abrasive established contact with the sample during the first 400 cycles only and that the used abrasive was employed to abrade the specimen surface subsequently in tests involving more than 400 cycles. Metallographically

polished specimens were loaded against the abrasive wheel with the help of a cantilever mechanism and allowed to move to-and-fro for a desired number of cycles. The samples were cleaned well and weighed prior to and after the wear tests. The material wear was computed by mass loss technique that was subsequently converted into volume loss. A Mettler microbalance with a precision level of 0.1 mg was used for weighing the samples.

2.4 Erosion-corrosion tests

Erosion-corrosion tests were carried out on 30 mm ×25 mm×3 mm rectangular samples using sample rotation technique. The test arrangement allowed samples, fixed on a (non conducting) disc at a radial distance of 40 mm, to rotate in the liquid (slurry) medium kept in a container. The speed of rotation employed in this study was 150 r/min corresponding to a linear velocity of 0.6 m/s. Three test environments were employed for conducting the erosion-corrosion tests that comprised of aqueous solutions of (a) 12% NaCl (mass fraction), (b) 25% urea and (c) 25% diammonium phosphate (DAP). Each of the solutions was mixed with 1.5% sub-angular silica sand particles (size: 1.5−2.0 mm) in order to prevent surface from passivation on the samples and produce additional erosive action. The test duration was varied in the range of 2−6 h. The Mettler microbalance having the precision level of 0.1 mg was used for weighing the samples prior to and after testing. The reported data represents an average of two observations.

3 Results

3.1 Microstructure

Figure 2 shows the microstructural features of the as-cast Al samples. Dendritic nature of grains of Al may be noted in Fig. 2(a), while a magnified view clearly reveals the grains along with intermetallic compounds (Fig. 2(b), regions marked by *A* and arrow respectively). The microstructural features of Al−Si (LM6) alloy are shown in Fig. 3. The as-cast alloy shows primary Al and eutectic Si particles (Fig. 3(a), regions marked by *A* and *B* respectively). A magnified view delineates long needle-like eutectic Si particles (Fig. 3(b)). T6 heat treated samples of the LM6 alloy show morphological alterations in the eutectic Si particles from long needle-like in the as-cast condition (Fig. 3(b)) to spheroidal when the ageing duration is varied in the range of 3−11 h (Figs. 3(c)−(e)). Limited coarsening of the Si particles with increasing ageing duration is also observed (Fig. 3(e) vs (c)).

3.2 Mechanical properties

Figure 4 shows the hardness, tensile strength and elongation of the Al−Si (LM6) alloy as a function of ageing duration. Zero on the ageing duration axis corresponds to the as-cast alloy. Properties of Al samples are also shown in the figure. The as-cast LM6 alloy attains higher hardness and strength but less elongation over the as-cast Al samples. Further, increasing ageing duration during the T6 heat treatment brings about a marginal decrease in strength while hardness and elongation follow a reverse trend.

3.3 Abrasive wear behaviour

Figures 5 and 6 show the abrasive wear loss of the samples. The heat treated Al−Si alloy samples exhibit less wear loss than the as-cast alloy (Fig. 5). Also, increasing ageing duration does not affect the wear behaviour of the samples appreciably while the wear loss increases with the applied load and traversal distance. The wear loss vs traversal distance plot of the samples is shown in Fig. 6. The as-cast Al−Si alloy exhibits less wear loss as compared to the conventional Al samples. Also, T6 heat treatment leads to a further decrease in the

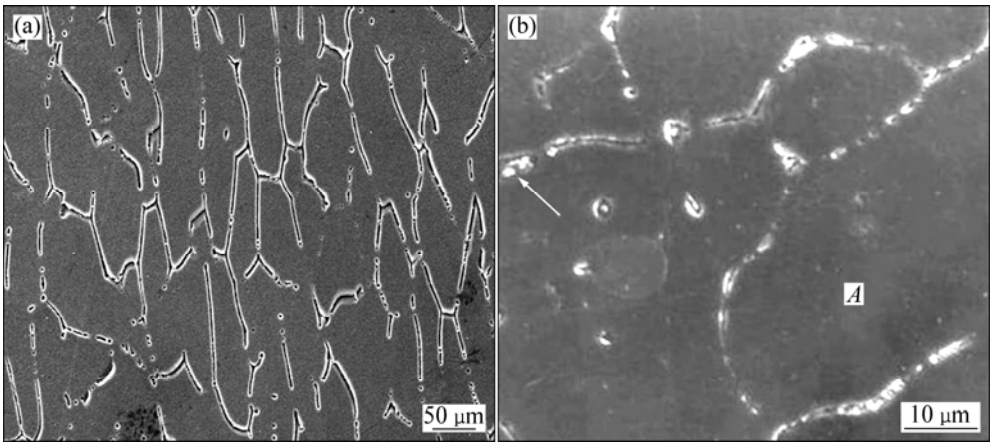

Fig. 2 SEM images of conventionally used commercial Al in as-cast condition: (a) General features; (b) Different microconstituents (*A*: Primary *α*; Arrow: Intermetallic compounds)

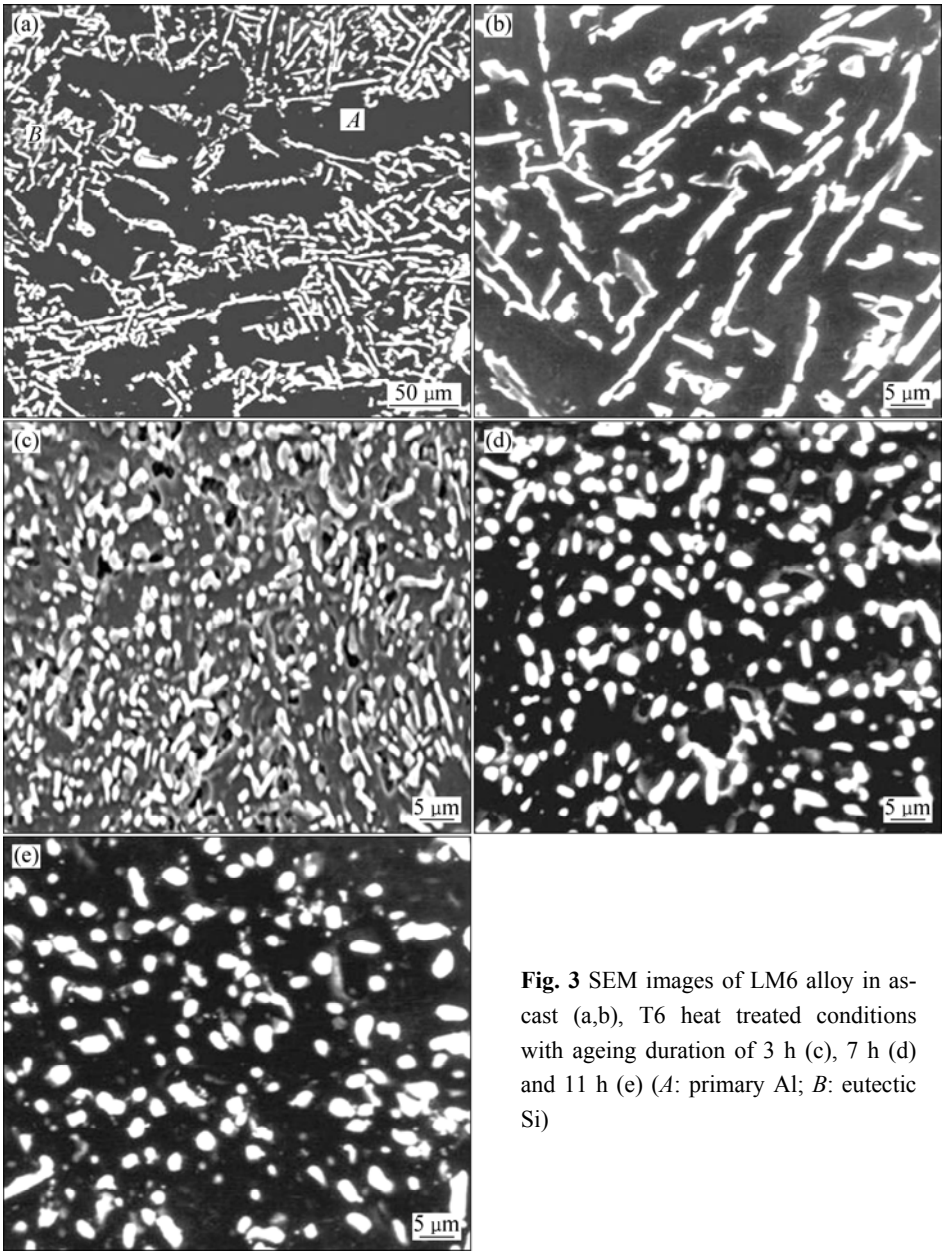

Fig. 3 SEM images of LM6 alloy in as-cast (a,b), T6 heat treated conditions with ageing duration of 3 h (c), 7 h (d) and 11 h (e) (*A*: primary Al; *B*: eutectic Si)

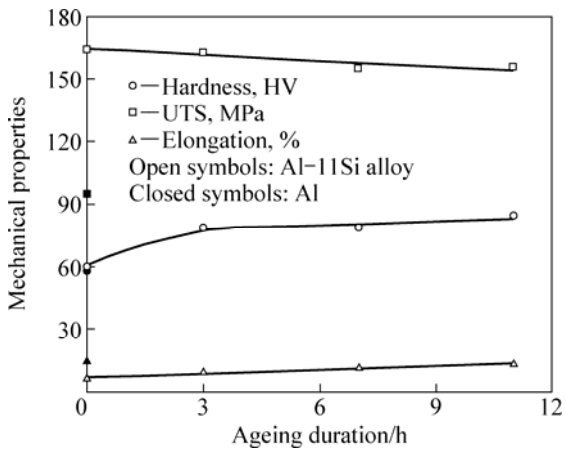

Fig. 4 Mechanical properties of Al−Si (LM6) alloy samples as function of ageing duration (Zero on the ageing duration axis represents as-cast alloy samples)

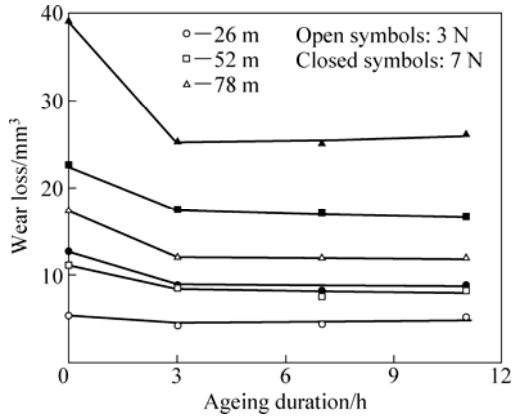

Fig. 5 Abrasive wear loss of Al−Si (LM6) alloy samples as a function of ageing duration at different applied loads and traversal distances (Zero on the ageing duration axis represents as-cast alloy samples)

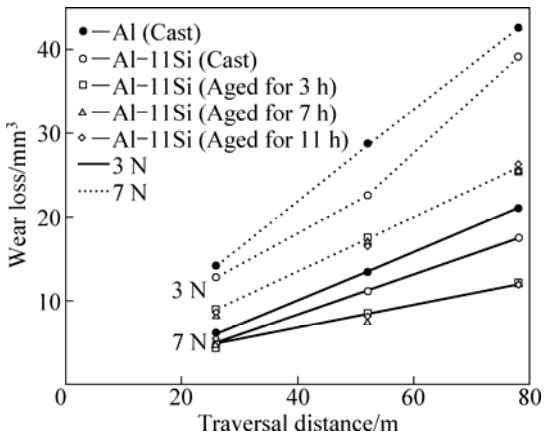

Fig. 6 Abrasive wear loss of as-cast and T6 heat treated Al−Si (LM6) alloy samples as a function of traversal distance at different applied loads and ageing durations

wear loss of the LM6 alloy while load and traversal distance produce a reverse effect.

3.4 Erosion-corrosion behaviour

The wear loss of the samples in the urea and DAP solutions was almost negligible, and in some cases even mass gain was noted, and hence not shown. The wear loss of the samples in the NaCl solution is shown as a function of test duration in Fig. 7. The effects of alloy composition and microstructural alterations brought about by T6 heat treatment on the performance of the samples are also shown in the figure. Increasing test duration caused the material loss to increase. Further, the as-cast Al−Si alloy exhibits substantially decreased material loss as compared to the conventionally used Al samples. Also, the T6 treated samples aged for 3 h show a mixed response while longer ageing duration leads to a greater extent of material loss when compared with the as-cast alloy.

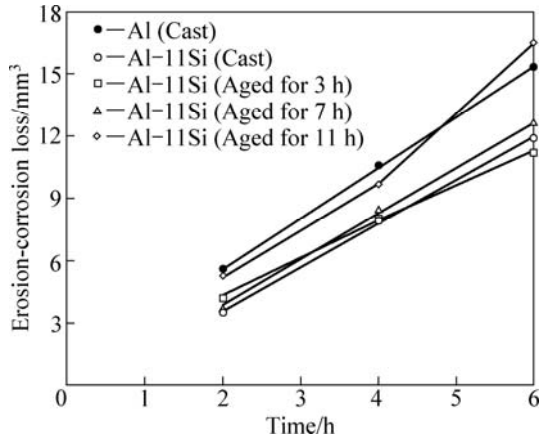

Fig. 7 Erosion-corrosion loss of as-cast and T6 heat treated Al−Si (LM6) alloy samples in NaCl solution as a function of test duration

3.5 Characteristics of abraded samples and abrasive medium

Figure 8 shows the abraded surfaces of the samples. The samples show well defined grooves in general (Fig. 8(a), region marked by single arrow). A few fragmented abrasive particles that got entrapped in the abraded surfaces in subsequent passes are also seen (Fig. 8(b), region marked by *A*). The grooves tend to be relatively less defined and shallower in the case of the as-cast Al−Si alloy (Fig. 8(c)) compared with the conventional Al (Fig. 8(a)). The hard Si phase is noticed to protrude on the wear surface during wear (Fig. 8(c), region marked by double arrow). The silicon particles also got exposed on the wear surface (Fig. 8(d), region marked by *B*). Features of the abraded surface of the Al−Si alloy aged for 3 h (Fig. 8(e)) was comparable to those of the as cast one (Fig. 8(c)).

Characteristics of subsurface regions of the abraded samples are presented in Fig. 9. Regions close to the wear surface undergo plastic deformation and reveal fragmented abrasive particles entrapped therein (Fig. 9(a), region marked by single arrow). A magnified view shows heavily deformed region attached to the bulk (Fig. 9(b), region marked *A*). Further, the microconstituents get refined significantly in the vicinity of the wear surface as compared to the ones below (Fig. 9(c), regions marked by *B* vs *C*). Some indication of material flow in the sliding direction is also noted (Fig. 9(c), region marked by double arrow). A typical example of fracturing of silicon particles is shown in Fig. 9(d) (region marked by triple arrow). The degree of attachment of regions to the bulk (Figs. 9(a) and (e), regions marked by *A*) is more in the case of conventional Al and aged Al−Si alloy as compared to that of the as-cast Al−Si alloy (Fig. 9(c)).

The abrasive medium prior to and after specimen testing is shown in Fig. 10. The debris is noted to be filled in the inter (abrasive) particle spacing and most of the abrasive particles are covered by the debris after abrasion testing (Fig. 10(b)). A magnified view shows that the debris consists of machining chips, flakes as well as fragmented Si/abrasive (SiC) particles (Figs. 10(c) and (d), regions marked by single arrow, A and double arrow, respectively). The abrasive particles got fractured and partially removed in the due course of testing (Fig. 10(e) and (f), regions marked by triple arrow and B, respectively).

4 Discussion

From microstructural standpoint, the conventionally used Al (Table 1) is basically a single phase material containing Al grains along with a limited quantity of intermetallic compounds (Fig. 2) in the presence of Cu,

Si and Fe. The Al−Si alloy used in this study (Table 1) comprises of Si in the range of eutectic composition [12,13]. In this case, since the ambient temperature solid solubility of Si in Al is negligibly small [12,13], the eutectic structure contains Al and Si phases (Fig. 3). Moreover, the eutectic structure in this alloy system is a divorced type [14] that shows a fairly random orientation of the eutectic Si particles in the as-cast Al matrix (Fig. 3(a)). It may be mentioned that some portion of the Si particles are expected to go to solid solution at the solutionizing temperature in view of enhanced solid solubility limit of Si in Al to the extent of ~1% at temperatures above 500 °C [12,13]. The dissolved Si gets precipitated as fine particles once the samples get cooled to ambient temperature after solutionizing. Sharp tips and edges of Si (Fig. 3(b)) give rise to higher concentration gradient and thus make the Si particles more prone to dissolution/fragmentation [15] during heat treatment. This also helps the Si particles to undergo the morphological change from long needle-like to spheroidal after heat treatment (Figs. 3(c)−(e) vs (b)). As far as the influence of needle-like morphology on mechanical properties is concerned, sharp tips and edges enhance the tendency of materials towards cracking [16]. Predominant cracking tendency leads to inferior mechanical properties since hard and strong phases like Si present in the material system give way prematurely in view of poor compatibility with the surrounding matrix and a faster nucleation and subsequent propagation of cracks [16]. Ductility in such cases becomes lower when spheroidal microconstituents are formed (Fig. 4). A marginal influence on strength as a result of the morphological modifications derived from the heat treatment (Fig. 4) could be attributed to the stress relief attained by the heat treated material [17]. An associated increase in the hardness of the Al−Si alloy after heat

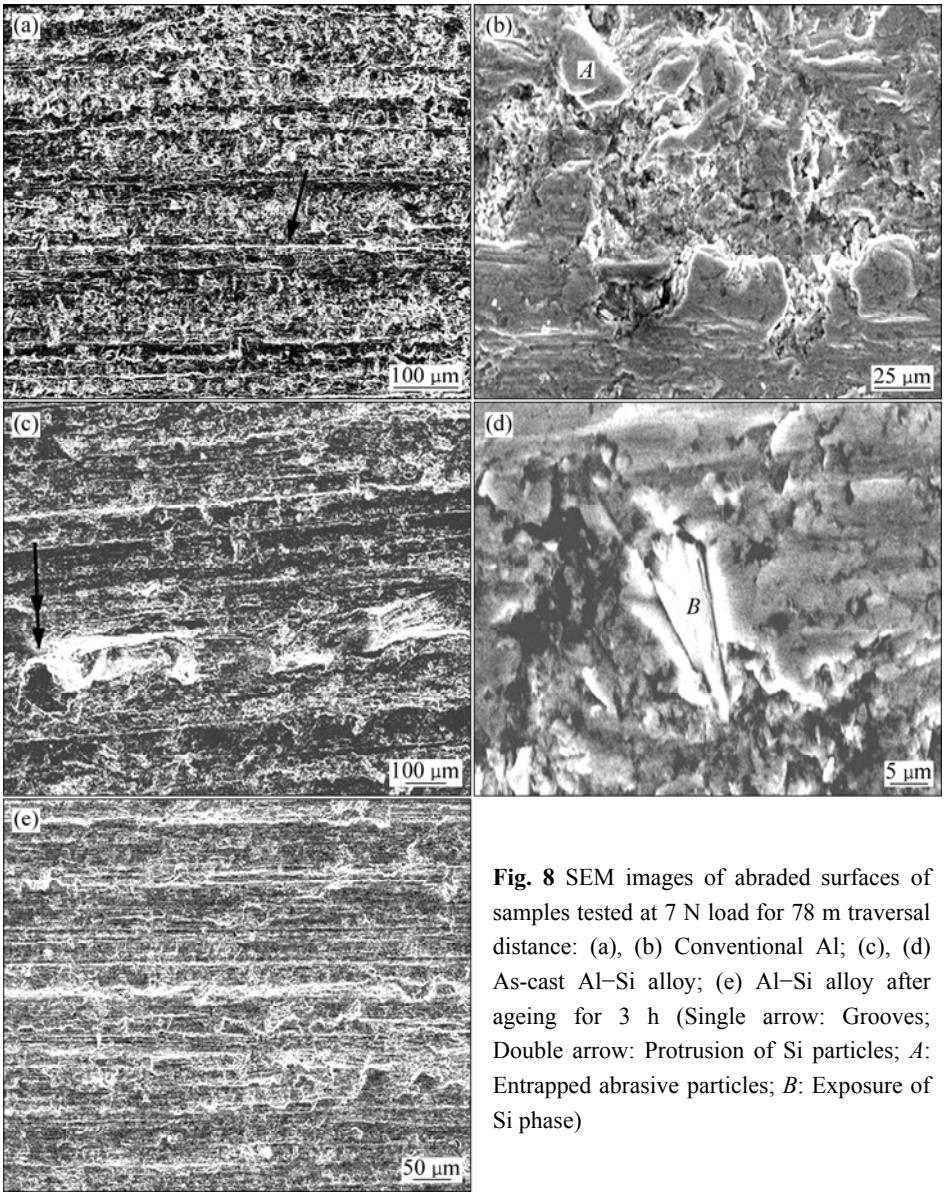

Fig. 8 SEM images of abraded surfaces of samples tested at 7 N load for 78 m traversal distance: (a), (b) Conventional Al; (c), (d) As-cast Al−Si alloy; (e) Al−Si alloy after ageing for 3 h (Single arrow: Grooves; Double arrow: Protrusion of Si particles; *A*: Entrapped abrasive particles; *B*: Exposure of Si phase)

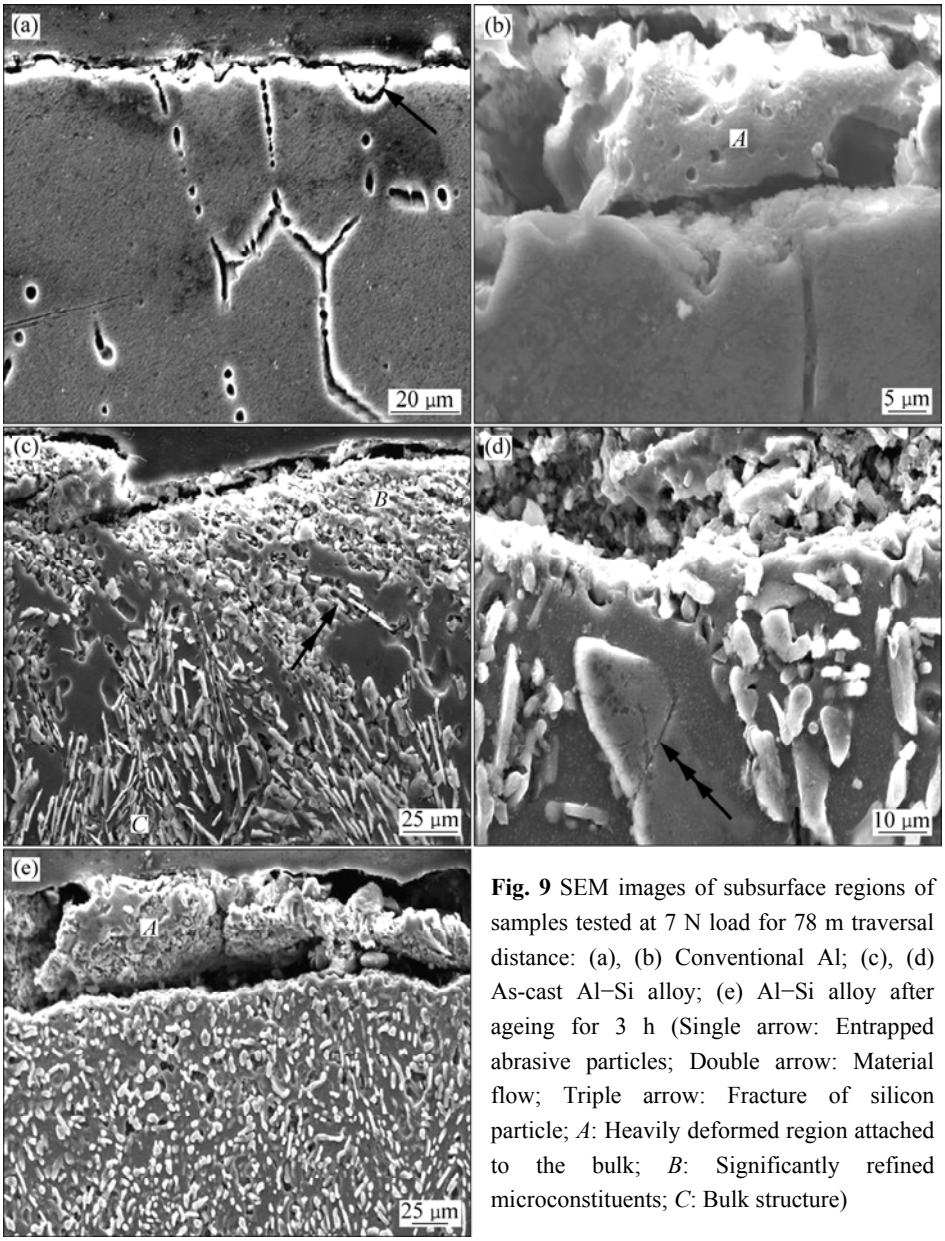

Fig. 9 SEM images of subsurface regions of samples tested at 7 N load for 78 m traversal distance: (a), (b) Conventional Al; (c), (d) As-cast Al−Si alloy; (e) Al−Si alloy after ageing for 3 h (Single arrow: Entrapped abrasive particles; Double arrow: Material flow; Triple arrow: Fracture of silicon particle; *A*: Heavily deformed region attached to the bulk; *B*: Significantly refined microconstituents; *C*: Bulk structure)

treatment (Fig. 4) could be attributed to the reduced cracking tendency in view of the presence of hard spheroidal Si particles that allow them to be retained by the Al matrix in view of suppressed cracking tendency and offer a more effective resistance [17] against the penetrating action of the hardness indenter. Higher hardness and strength of Si than that of Al enable the Al−Si alloy to display greater strength and hardness but lower ductility as compared to the conventional Al as shown in Fig. 4.

Higher hardness and greater strength of the Al−Si alloy cause its abrasive wear loss to reduce substantially when compared with the Al samples (Fig. 6). This is due to the protection offered by the Si particles to the softer and weaker Al phase against the penetrating action of the SiC abrasive particles [18]. Protrusion and/or exposure of Si particles on the abraded surface (Figs. 8(c) and (d), regions marked by double arrow and *B* respectively) further strengthen the view. Improved abrasive wear behaviour of the heat treated Al−Si alloy over that of the as-cast version (Fig. 5) could be attributed to the increasing ductility thereby causing decreasing cracking tendency of the material due to the formation of spheroidal Si particles after heat treatment (Figs. 3(c)−(e)). However, a marginal effect of morphological alteration with the increasing ageing duration (Fig. 3(d) vs (c)) results into an inappreciable change in the wear response of the heat treated Al−Si alloy (Fig. 5). Increasing wear loss with load could be attributed to the greater severity of wear condition due to a deeper penetration of the abrasive particles on the specimen surface [18,19], while a similar effect on the wear

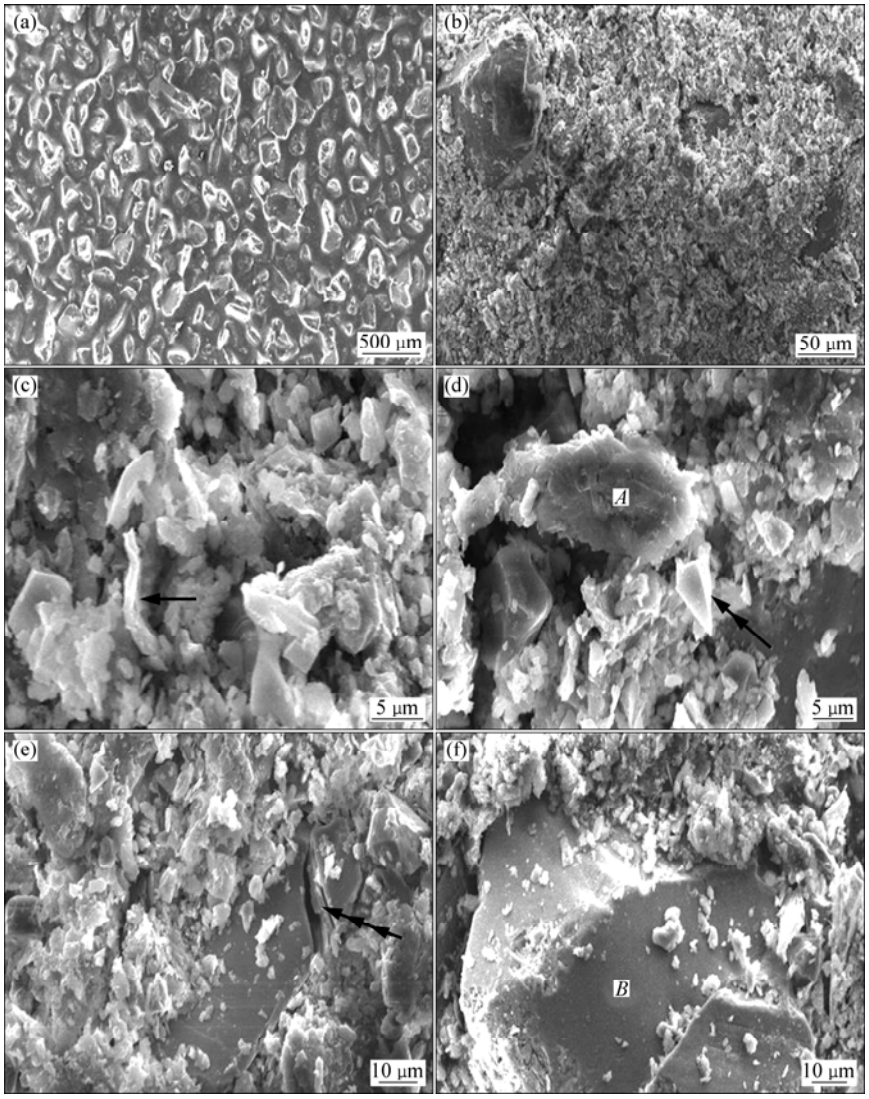

Fig. 10 SEM images of abrasive medium prior to (a) and after specimen testing at 7 N load for 78 m distance for Al (b) and Al−Si (c−f) alloy (Single arrow: Machining chip; *A*: Flake; Double arrow: Fragmented Si/abrasive (SiC) particles; Triple arrow: Fracture of abrasive particle; *B*: Partial removal of abrasive particle)

response with rising traversal distance may be a result of longer duration of contact of the abrasive with the specimen to cause material loss/damage (Fig. 5).

As far as the erosion-corrosion behaviour of the Al−Si alloy is concerned, counterbalancing effects of the Si particles, namely higher erosion and corrosion resistance leading to improved wear resistance and Si/Al-matrix interfacial attack of the medium causing an adverse influence on the response [12,20−24], need to be taken into account. Available information suggests that Si is less prone to corrosive attack as compared to Al by a medium like NaCl solution, while higher hardness and strength of Si enables to resist the erosive action of the medium [12,20−24]. It may also be mentioned that the T6 heat treatment brings about a remarkable alteration in the morphology of the eutectic Si phase from needle-like sharp tips in the as-cast condition (Fig. 3(b)) to spheroidal one (Figs. 3(c)−(e)). This leads to an increase in the Si/Al matrix interfacial area and hence more severe interfacial attack [20−22] by the medium after heat treatment. Accordingly, a reduction in the erosive-corrosive wear loss of the Al−Si alloy over that of Al (Fig. 7) suggests the higher erosion and corrosion resistance (inverse of material loss) of Si particles to dominate over the Al matrix/Si interfacial attack of the medium. On the contrary, deterioration in the wear performance of the heat treated Al−Si alloy samples over that of the as-cast one (Fig. 7) signifies the predominant role played by the interfacial attack of the medium. The increased severity of erosion-corrosion loss of the T6 heat treated samples in general (Fig. 7) may be due to the predominant adverse effect of Si/Al matrix interfacial attack of the medium; the latter gets aggravated further through the impinging action of the sand particles

suspended in the medium [20−22]. This also suggests that the erosion-corrosion behaviour of the Al−Si alloy in the NaCl solution is greatly controlled by the morphological alterations in Si brought about by the heat treatment (Figs. 3(c) and (d) vs (b)). No material loss during the erosion-corrosion testing of the samples in the urea and DAP fertilizer solutions could be attributed to the fact that both DAP and urea are basically nitrogenous fertilizers with organic compounds that make the electrolytic dissolution of aluminum and its alloying elements sluggish.

Well defined grooves on the abraded surfaces (Fig. 8(a), region marked by arrow) are produced due to the cutting action of the hard abrasive particles [18,19]. Machining chips (Fig. 10(c), region marked by single arrow) are produced in such cases [25]. Hard debris/ abrasive particles that get entrapped on the abraded surface (Fig. 8(b), region marked by *A*) after their fragmentation (Fig. 10(d), region marked by double arrow) behave as a cutting tool and protect the specimen surface against further damaging action of the abrasive. Exposure and/or protrusion of hard microconstituents on the wear surface (Figs. 8(c) and (d), regions marked by double arrow and *B* respectively) also protect the specimen surface, leading to decreased wear loss [18,19]. Flake type debris is produced by the ploughing action of the abrasive particles [25]. Prow regions of the ploughed area work harden and fragment in the due course of abrasion ultimately leading to the generation of the flakes. Delamination of material due to joining of microcracks on and below the wear surface has also been suggested to form flaky debris [26].

Changes in the microstructural features of the samples below the abraded surfaces result from the varying degree of plastic deformation experienced by the regions at different depths [16,17]. It may be mentioned that the region in the nearest vicinity of the wear surface (top) experiences the severe deformation, leading to the generation of the finest microconstituents (Fig. 9(c), regions marked by *B*). This is followed by some indication of material flow in the sliding direction, indicating relatively little severity of wear induced deformation in the region below (Fig. 9(c), region marked by double arrow). The region much below the wear surface remaining practically unaffected displays features (Fig. 9(c), region marked by *C*) close to that of the normal bulk structure (Figs. 3(a) and (b)). Cracking of Si particles below the wear surface (Fig. 9(d), region marked by triple arrow) suggests its participation in load transfer and thus resisting the penetrating action of the abrasive particles.

During abrasion, the debris generated is first entrapped on the abrasive surface. This process is known as clogging and most potential sites for this purpose are the inter(abrasive) particle spacing (Fig. 10(b)). Some of the debris also gets deposited on the abrasive particles thus producing a capping action (Fig. 10(b)). Blunting (attrition) of the abrasive also occurs during abrasion. Cutting efficiency of the abrasive particles deteriorates as a result of clogging, capping and attrition since the mentioned processes reduce the depth of penetration of the (abrasive) particles [27]. Fragmentation/partial removal of the abrasive particles (Fig. 10(f), region marked by *B*) produces a mixed influence on the severity of their damaging action. For example, fragmentation leads to the generation of many newer sharp tips and edges causing improved cutting efficiency while their (partial) removal produces a reverse effect.

5 Conclusions

1) The as-cast Al−Si (LM6) alloy revealed needle-like eutectic Si particles and Al. T6 heat treatment changed the morphology of the Si particles to spheroidal and also improved the homogeneity of their distribution in the Al matrix.

2) The as-cast Al−Si alloy exhibited higher hardness, tensile strength and elongation as compared to the conventional Al samples. T6 heat treatment brought about improved hardness and elongation along with a marginal influence on the strength of Al−Si alloy.

3) Abrasive wear resistance (inverse of material loss) of the Al−Si alloy was higher than that of the conventional Al samples. T6 heat treatment brought about a further improvement in the wear performance of Al−Si alloy. However, increasing ageing duration did not produce any appreciable effect on the abrasive wear behaviour. Also, the wear response of the samples deteriorated with increasing traversal distance and applied load.

4) Erosion-corrosion resistance of the as-cast Al−Si alloy was observed to be superior to that of the conventional Al samples. On the contrary, the wear response of the Al−Si alloy deteriorated after heat treatment. Also, practically no material loss was noticed during erosion-corrosion in the DAP and urea fertilizer solutions.

5) Improved performance of the as-cast as well as heat treated Al−Si (LM6) alloy in terms of hardness, elongation, strength and abrasion and erosion-corrosion wear resistance over that of the conventional Al strongly suggests the Al−Si alloy to have potential to replace the latter in agricultural applications like sowing.

6) Cutting and ploughing actions of the abrasive particles were observed to be responsible for the abrasion loss. Capping, clogging and attrition led to reduce the cutting efficiency of the abrasive particles. Fracturing and partial removal of the abrasive particles produced a mixed influence on the abrasive wear response of the samples.

References

[1] VERMA S R. Seed-cum-fertilizer drills in India [C]//Proceedings of the International Conference on Small Farm Equipment for Developing Countries—Past Experiences and Future Priorities. Los Banos, Philippines: International Rice Research Institute, 1986: 121-135.

[2] EDWARDS J D. The properties of pure aluminum [J]. Transactions of the American Electrochemical Society, 1925, 47: 287−300.

[3] PORTER F C, HODDEN S E. Nodular pitting of aluminum alloys [J]. Journal of Applied Chemistry, 1953, 3: 385−409.

[4] SRIVASTAVA N S L, DUBEY A K. Development and field evaluation of an animal drawn three row seed cum fertilizer drill cum two-row planter [C]//Proceedings of the Silver Jubilee Convention of the Indian Society of Agricultural Engineers. Bhopal, India: Central Institute of Agricultural Engineering, 1985: 11−32.

[5] BROWN R H, FLINK W L, HUNTER M S. Measurement of irreversible potential as a metallurgical tool [J]. Transactions of the American Institute of Metallurgical Engineers, 1941, 143: 115−123.

[6] RIGNEY D A. Fundamentals of friction and wear [M]. American Society for Metals, 1981: 145−163, 358−370.

[7] SICHA W E. Aluminum base casting alloys [M]//Cast Metals Handbook. American Foundrymen's Society, 1957: 254−270.

[8] LANCER M V. Metallurgy of aluminum alloys [M]. 2nd ed. London: Chapman & Hall, 1967: 169−196.

[9] MONDOLFO L F. Aluminium alloys: Structure and properties [M]. 1st ed. London: Butterworths Ltd, 1976: 368.

[10] TALBOT D E J, GRANGER D A. Secondary hydrogen porosity in aluminum alloys [J]. Journal of Institute of Metals, 1964, 92: 290−297.

[11] GUPTA A K, TIWARI S N, MALHOTRA S L. Volumetric contractions accompanying cooling and freezing in Al−Cu and Al−Si alloys [J]. The British Foundryman, 1992, 20: 192−198.

[12] POLMEAR I J. Light alloys: Metallurgy of light metals [M]. London: Edward Arnold Publishers Ltd, 1981: 110−126.

[13] BRANDES E A. Smithells metals reference book [M]. 6th ed. London: Butterworths Ltd, 1983: 370−801.

[14] DAHLE A K, NOGITA K, MCDONALD S D, ZINDEL J W, HOGAN L M. Eutectic nucleation and growth in hypoeutectic Al-Si alloys at different strontium levels [J]. Metallurgical and Materials Transactions A, 2001, 32: 949−960.

[15] CHRISTIAN J W. The theory of transformations in metals and alloys, part I: Equilibrium and general kinetic theory [M]. 2nd ed. USA: Pergman Press, 1981: 169.

[16] PRASAD B K, PATWARDHAN A K, YEGNESWARAN A H. Dry sliding wear characteristics of some zinc-aluminium alloys: A comparative study with a bearing bronze at a slow speed [J]. Wear, 1996, 199: 142−151.

[17] PRASAD B K. Dry sliding wear behaviour of zinc-based alloy: Influence of heat treatment and sliding speed and pressure [J]. Materials Science and Technology, 1997, 13: 928−936.

[18] PRASAD B K, VENKAT K, MODI O P, YEGNESWARAN A H. Influence of the size and morphology of silicon particles on the physical, mechanical and wear properties of aluminium-silicon alloys [J]. Journal of Materials Science Letters, 1996, 15: 1773−1776.

[19] PRASAD B K, JHA A K, MODI O P, DAS S, YEGNESWARAN A H. Abrasive wear characteristics of a Zn−37.2Al−2.5Cu−0.2Mg alloy dispersed with silicon carbide particles [J]. Materials Transactions of the Japan Institute of Metals, 1995, 36: 1048−1057.

[20] PROTOPOPOFF E, MARCUS P. Handbook of metals corrosion fundamentals, testing and protection [M]. Materials Park, Ohio: ASM, 2003: 8−12.

[21] PRASAD B K, MODI O P. Slurry wear characteristics of zinc-based alloys: Effects of sand content of slurry, silicon addition to alloy system and traversal distance [J]. Transactions of Nonferrous Metals Society of China, 2009, 19: 277−286.

[22] PRASAD B K, MODI O P, YEGNESWARAN A H. Wear behaviour of zinc-based alloys as influenced by alloy composition, nature of the slurry and traversal distance [J]. Wear, 2008, 264: 990−1001.

[23] MODI O P, SAXENA M, PRASAD B K, JHA A K, DAS S, YEGNESWARAN A H. The role of alloy matrix and dispersoid on the corrosion behaviour of cast aluminium alloy composites [J]. Corrosion, 1998, 54: 129−134.

[24] SUMMERSAN J J, SPROWLS D O. Corrosion behaviour of Al alloys [C]// STARKE E A Jr, SANDERS T H Jr. Proceedings of the International Conference on Aluminium Alloys: Their Physical and Mechanical Properties. Charlottesville, Virginia, 1986: 575−631.

[25] MURRAY M J, MUTTON P J, WATTSON J D. Abrasive wear mechanisms in steels [J]. Journal of Lubrication Technology, 1982, 104: 9−16.

[26] SUH N P. An overview of the delamination theory [J]. Wear, 1977, 44: 1−16.

[27] PRASAD B K. Abrasive wear characteristics of a zinc-based alloy and zinc alloy/SiC composite [J]. Wear, 2002, 252: 250−263.

T6 热处理对共晶 Al−Si 合金力学性能、耐磨和抗蚀性能的影响

A. K. GUPTA[1], B. K. PRASAD[1], R. K. PAJNOO[2], S. DAS[1]

1. CSIR - Advanced Materials and Processes Research Institute, Bhopal-462026, India;
2. Central Institute of Agricultural Engineering (ICAR), Bhopal-462028, India

摘　要：对共晶 Al−Si 合金的耐磨、抗蚀性能进行研究。通过控制 T6 热处理参数来改变共晶 Al−Si 合金的组织，研究组织变化对合金的硬度、强度和拉伸性能的影响，以及对抗冲蚀和腐蚀性能的影响。采用 Al−Si 合金制备了一典型的农机零部件。并将 Al−Si 合金与常用的农机用铝材的性能进行比较。结果表明，合金的化学成分、显微组织、载荷、滑动距离和试验环境对材料的耐磨、抗冲蚀和腐蚀性能有很大的影响。铸态 Al−Si 合金的性能要明显优于传统的铝材，而且 T6 热处理能够改善 Al−Si 合金的性能。因此，可采用 Al−Si 合金来替代传统的铝材制造农机。

关键词：Al−Si 合金；热处理；磨损；冲蚀；腐蚀

(Edited by YUAN Sai-qian)